



Biomedical Science  
Faculty of Health and Society  
Malmö University  
SE-205 06 Malmö  
Sweden

Master programme in Biomedical Surface Science  
<http://edu.mah.se/en/Program/VABSE>

Master degree thesis, 30 ECTS  
Examensarbete, 30 hp

## **Investigation of vitamin K interaction and transdermal delivery at skin barriers: study using K<sub>4</sub> model**

Alberta Agyemang

SUPERVISOR:  
Prof. Tautgirdas Ruzgas

2021-08-18

## ABSTRACT

Vitamin K is a fat-soluble compound which is synthesized by the gut microbiota and produced in many tissues within the body. Considering its role in the liver as a cofactor for gamma carboxylase enzymes, treatment of dark circles and pigments under the eye among others. It is clear that in some circumstances vitamin K has to cross biological barriers, particularly, when the vitamin is produced by microbiota in the intestine or applied topically on skin. Thus, it is important to develop methods that allow studies of vitamin K permeability through skin. In this thesis work we aim to study interaction of vitamin K with the skin including its participation in redox reactions and transdermal permeability. Taking into account that transdermal permeability is strongly limited for high molecular weight compounds, i.e., compounds with higher than 500 Da, the study was conducted with vitamin K of lower molecular weight. Specifically, vitamin K4 model, i.e., 1,4-dihydroxy-2-naphthoic acid, with molecular weight of 204g/mol. Vitamin K4 is suitable for this kind of study, because it can work as reducing (antioxidant) compound as well as has relatively beneficial physicochemical characteristics for transdermal permeability. Permeability studies were conducted with skin covered oxygen electrode and Franz diffusion cell. Data from measurements were analyzed to estimate diffusion coefficients, apparent Michaelis-Menten constants and flux of a vitamin K4 model whilst contribution of different permeability pathways was determined theoretically.

**Keywords:** Vitamin K4, diffusion coefficient, Michaelis-Menten constant, flux

This master thesis has been defended on August 18, 2021 at the Faculty of Health and Society, Malmö University.

Opponent: Assoc. Prof. Sebastian Björklund  
Faculty of Health and Society  
Department of Biomedical Science  
Malmö University

Examiner: Prof. Sergey Shleev  
Biomedical Science  
Faculty of Health and Society  
Malmö University

# TABLE OF CONTENTS

<b>INTRODUCTION.</b>	<b>4</b>
Contribution of microbiota in vitamin K production at biobarriers.	6
Benefits of topical vitamin K.	6
Aim	7
<b>MATERIALS</b>	<b>8</b>
<b>METHODS</b>	<b>8</b>
Skin preparation	8
UV-VIS Spectrophotometry	8
Amperometric measurements with skin covered oxygen electrode.	8
Franz diffusion cell	9
<b>RESULTS.</b>	<b>10</b>
UV-VIS Spectrophotometry	10
Determination of diffusion coefficients and lag times for hydrogen peroxide and 1,4-dihydroxy-2-naphthoic acid	11
Determination of Michaelis-Menten constants for hydrogen peroxide and 1,4-dihydroxy-2 naphthoic acid	13
Determination of flux	17
<b>DISCUSSION</b>	<b>18</b>
<b>CONCLUSION</b>	<b>20</b>
<b>ACKNOWLEDGEMENTS</b>	<b>21</b>
<b>REFERENCES</b>	<b>22</b>
<b>APPENDIX</b>	<b>24</b>
Determination of lag times and diffusion coefficients	25
Determination of Michaelis-Menten constants $KM_{APP}$	27
Determination of flux	32
Theoretical flux	33

## INTRODUCTION.

Vitamin K a fat-soluble vitamin is an essential cofactor for the carboxylation of glutamyl residues to form gamma-carboxyglutamyl residues in blood clotting proteins (Shearer, 2009, Pazyar et al., 2019). Vitamin K dependent proteins involved in blood coagulation mechanisms are synthesized in the liver (Figure 1).

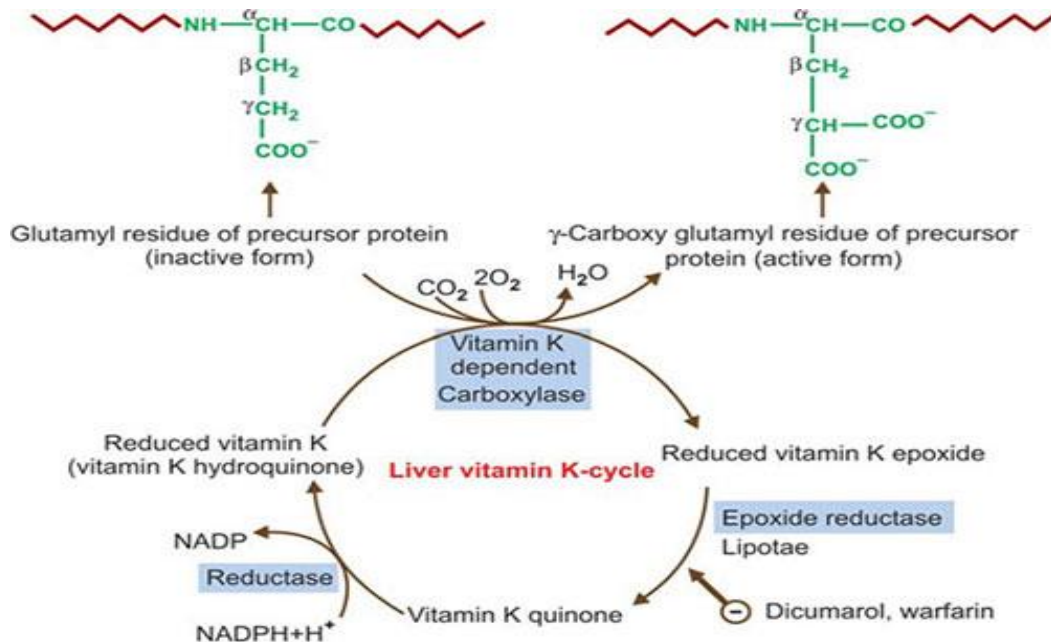
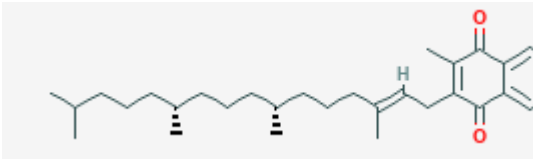
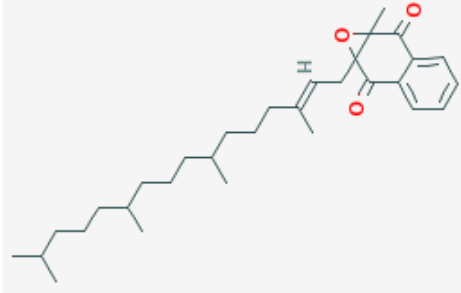
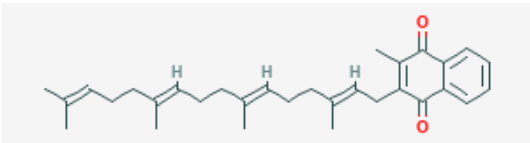
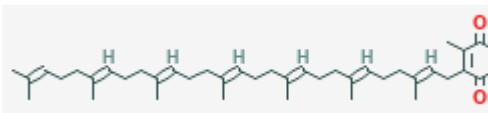
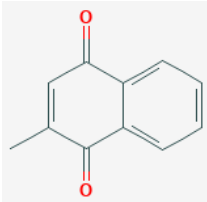
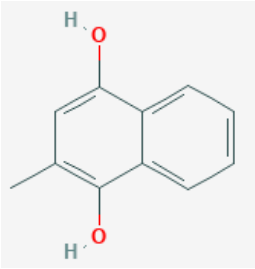
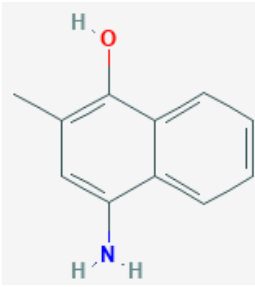
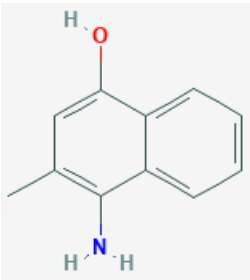


Figure 1. Vitamin K cycle in the liver (Pankaja, 2016).

In the liver vitamin K epoxide is reduced by epoxide reductase to vitamin K quinone and subsequently to vitamin K hydroquinone. Vitamin K antagonists such as warfarin, dicumarol inhibits vitamin K epoxide reductase, an enzyme important for blood coagulation via vitamin K cycle (Figure 1). Naturally vitamin K occurs in two main forms, the phylloquinone (vitamin K1) and the menaquinones (vitamin K2). Their chemical formulas are presented in Table 1.

Table 1. Chemical structures of vitamin K taken from PubChem.

	
<p>Phylloquinone K1</p>	<p>Phylloquinone oxide, vitamin K10</p>
	
<p>Menaquinone-4, vitamin K2 family</p>	<p>Menaquinone-7, vitamin K2 family</p>
	
<p>Menadione, Vitamin K3</p>	<p>Menadiol, vitamin K4</p>
	
<p>Vitamin K5</p>	<p>Vitamin K7</p>

Phylloquinone are found in abundance in green leafy vegetables including spinach, cabbage, and lettuce. Menaquinones are present in fermented foods including cheese and can also be synthesized by the gut microbiota. Vitamin K

forms have a common 2-methyl-1,4-naphthoquinone ring structure (K3 in Table 1). However, they differ from each other in the length and degree of saturation of the polyisoprenoid side chain attached to the 3-position (Schurgers and Vermeer, 2000). The phyloquinones have phytyl side chains whereas the menaquinones have side chains of repeating unsaturated 5-carbon prenyl units. The classification of the menaquinones depends on the number of prenyl units which is between 4 to 13. The number of units is given in a suffix (-*n*), that is, menaquinone-*n* and often abbreviated as MK-*n* (World Health Organization, 2004, Hill, 1997). Menaquinone-4 and menaquinone-7 are the commonly studied types of menaquinones.

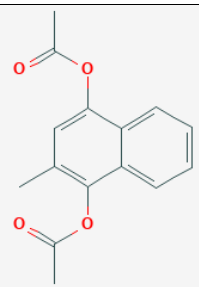
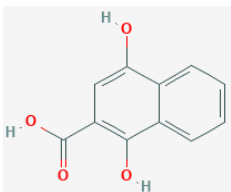
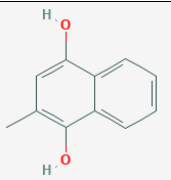
### **Contribution of microbiota in vitamin K production at biobarriers.**

The gut microbiota can synthesize certain vitamins, notably vitamin K, and B group vitamins including biotin, cobalamin, folates, nicotinic acid (Rowland et al., 2018). This is supported by studies performed by Gustafsson et al. (1962) where germfree rats reared without a dietary supplement of vitamin K have low prothrombin levels and develop hemorrhages, while their conventional counterparts have normal prothrombin levels and normal clotting activity. Additional studies conducted by LeBlanc et al. (2013) where microbiomes of the gut microbiota were found to have an abundance of clustered orthologous groups which are involved in the synthesis of deoxyxylulose-5-phosphate, a precursor of a certain class of vitamin B, thiamine and pyridoxine, further corroborates claim by Gustafsson et al.

### **Benefits of topical vitamin K.**

Topical Vitamin K may promote wound healing activity, probably due to its ability to significantly increase the rate of wound contraction, enhancement of the epithelialization period and generation of fibroblasts cells and blood vessels (Pazyar et al., 2019). In addition, vitamin K has been thought of to promote wound healing due to its involvement as a cofactor of carboxyglutamic acid in blood coagulation mechanisms. Due to its redox properties, vitamin K has been studied to have antioxidant properties which eliminates reactive oxygen species as reactive oxygen species can delay wound healing (ibid). Vitamin K prophylaxis can prevent vitamin K deficiency bleeding (Schulte et al., 2014). Low concentration of vitamin K in breast milk, low amount of vitamin K in the liver of neonates and poor transport from mother to fetus through the placenta can result in the fatal bleeding disorder, vitamin K deficiency bleeding, which was previously termed as the hemorrhagic disease of the newborn. The World Health Organization recommends that newborns receive 1 mg intramuscular (IM) injection of vitamin K at birth (Hutton et al., 2018). Dietary supplements of vitamin K increases bone health, and this mechanism is by increasing osteocalcin concentration during bone mineralization. Osteocalcin is a vitamin K dependent protein with three gamma carboxyglutamic acid motifs. This protein is non-collagenous and is synthesized by osteoblasts. Osteocalcin in the presence of calcium, facilitates mineral deposition and bone remodeling (Razzaque, 2011). Dark circles and pigments under the eyes can be improved when vitamin K is used in combination with vitamin C, E and retinol. Aside allergic reactions no other known side effects of topical vitamin K have been established. However, vitamin K should be used with caution in patients who are taking warfarin, a known vitamin K antagonist as its effects can be counteracted by vitamin K.

*Table 2.* Physicochemical characteristics of vitamin K4, i.e., menadiol and related compounds as alternatives for menadiol. The characteristics can be found in the Pubchem database.

Physicochemical characteristics	Chemical Structure
Chemical name: Menadiol diacetate, vitamin K4 Molecular weight: 258.27 g/mol Partition coefficient, log P: 3	
Chemical name: 1,4-Dihydroxy-2-naphthoic acid Molecular weight: 204.18 g/mol Partition coefficient, log P: 2.5	
Chemical name: 2-Methylnaphthalene-1,4-diol, menadiol Molecular weight: 174.2 g/mol Partition coefficient, log P: 2.8 (This might be not available for purchase)	

Considering the significant benefits of vitamin K, it is important to develop in - vitro models for research to understand the mechanisms of its interaction including partition, diffusion, and kinetics of interactions at skin barriers to develop technologies to ensure efficient drug delivery. Taking into account that transdermal permeability is strongly limited for high molecular weight compound, i.e., compounds with molecular weight higher than 500 Da, the planned study was conducted with vitamin K of lower molecular weight, specifically, vitamin K4 model (see Table 1), i.e., menadiol. This model compound is suitable for this kind of study because it can act as a reducing (antioxidant) compound as well as having relatively suitable physicochemical characteristics for transdermal permeability such as molecular weight below 500Da, partition coefficient between 1 and 3, low effective dose and therapeutic index. (see Table 2).

## Aim

From the review of the role and importance of vitamin K as a cofactor of carboxyglutamic acid in the blood coagulation cascade, prevention of vitamin K deficiency bleeding in neonates, and the contributions of the gut microbiota in the synthesis of vitamin K we have been interested to develop methods for investigating vitamin K permeability in the skin and its involvement in redox-antioxidant reactions in the skin. For these reasons we have done relevant experiments using skin covered oxygen electrodes and Franz diffusion cells.

## MATERIALS

1,4-dihydroxy-2-naphthoic acid was purchased from Sigma Aldrich(Hesse, Germany), phosphate buffered saline tablets and ethylenediaminetetraacetic acid tablets were purchased from Sigma Aldrich(St. Louis,Missouri), hydrogen peroxide was purchased from Sigma Aldrich(Kandel, Germany), potassium chloride was purchased from Sigma Aldrich (St. Louis, Missouri), porcine ears were purchased from a local abattoir(illstorp,Sweden), Oxygen electrode consisting of a platinum (Pt) electrode and an internal Ag/AgCl reference electrode purchased from Optronika UAB (Vilnius, Lithuania), AMEL model 2059 potentiostat was purchased from AMEL (Milano, Italy), alumina suspension was obtained from Buehler (Lake Bluff, Illinois). All solutions were prepared using water which has been purified by Milli-Q system purchased from Merck Millipore (Billerica, Massachusetts).

## METHODS

### Skin preparation

Porcine ears were used as skin membrane during the study. The ears were stored at -80 °C prior to use. Skin membranes were prepared by washing the defrosted ears with cold water and cut into strips. The skin strips were shaved and sliced with a dermatome to a thickness of 0.5 mm. Circular membranes of 16 mm diameter were punched out of the skin strips and placed onto an aluminum foil and stored at -18 °C. The skin membranes were thawed in PBS before use and skin membranes from different pigs were used for the experiments.

### UV-VIS Spectrophotometry

0.00204 g of 1,4-dihydroxy-2-naphthoic acid was weighed and dissolved in 5 mL of phosphate buffered saline, PBS and 5 mM ethylenediaminetetraacetic acid, EDTA to aid the dissolution of 1,4-dihydroxy-2-naphthoic acid and was stored in a dark place. This stock solution was of 2 mM concentration. The absorption spectrum for 1,4-dihydroxy-2-naphthoic acid in PBS with 5mM EDTA using quartz cuvettes was recorded between 250 and 650nm. A calibration curve of measured absorbances against concentrations of 0.02, 0.04, 0.06, 0.08 and 0.01mM was thus obtained for 1,4-dihydroxy-2-naphthoic acid.

### Amperometric measurements with skin covered oxygen electrode.

The surface of the platinum cathode of the oxygen electrode was polished with alumina and rinsed with deionized water. The oxygen electrode was assembled by covering the platinum cathode with a 5 µm thick Teflon<sup>+</sup> membrane and a skin patch with a thickness of 500 µm. The cap of the electrode was filled with 500 mL of saturated potassium chloride and immersed into an electrochemical cell filled with 10 mL of buffer, PBS. Amperometric measurements were performed by applying -0.7V vs Ag/AgCl to reduce O<sub>2</sub> to H<sub>2</sub>O<sub>2</sub> according to  $O_2 + 4e^- + 4H^+ \rightarrow 2H_2O$  the platinum cathode of the oxygen electrode under constant stirring. A baseline current which is the current response of the skin covered oxygen



electrode was recorded in PBS with a potentiostat. 100  $\mu$ l of 100 mM hydrogen peroxide was injected into the cell and current responses were measured. At each hour 100  $\mu$ L of 1,4-dihydroxy-2-naphthoic acid was added into the electrochemical cell and current responses were measured. Data was processed to estimate lag times and diffusion coefficients of hydrogen peroxide and 1,4-dihydroxy-2-naphthoic acid. This procedure was repeated for the determination of Michaelis-Menten constants where current responses were measured upon five additions of 100  $\mu$ L of 100 mM hydrogen peroxide and five additions of 100  $\mu$ L of 1,4-dihydroxy-2-naphthoic acid. Data was processed to estimate the maximum currents of the reaction and Michaelis-Menten constants for both hydrogen peroxide and 1,4-dihydroxy-2-naphthoic acid.

### **Franz diffusion cell**

Permeation of 1,4-dihydroxy-2-naphthoic acid was investigated using Franz diffusion cells. A magnetic stirrer was placed in the receptor chamber for agitation and was filled with 6 mL of PBS. A porcine inner ear of thickness 9 mm was thawed in PBS and mounted on the receptor chamber with the stratum corneum facing the donor chamber. The set up was tilted to allow air bubbles to escape from the sampling port. The donor chamber was clamped onto the receptor chamber and filled with 0.6 mL of 2 mM 1,4-dihydroxy-2-naphthoic acid. At hourly time interval 300  $\mu$ L of 1,4-dihydroxy-2-naphthoic acid was sampled from the receptor chamber with a glass syringe for UV assay and replaced with 300  $\mu$ L of PBS. Following UV analysis an absorption spectrum of measured absorbances as a function of concentrations was obtained.

# RESULTS.

## UV-VIS Spectrophotometry

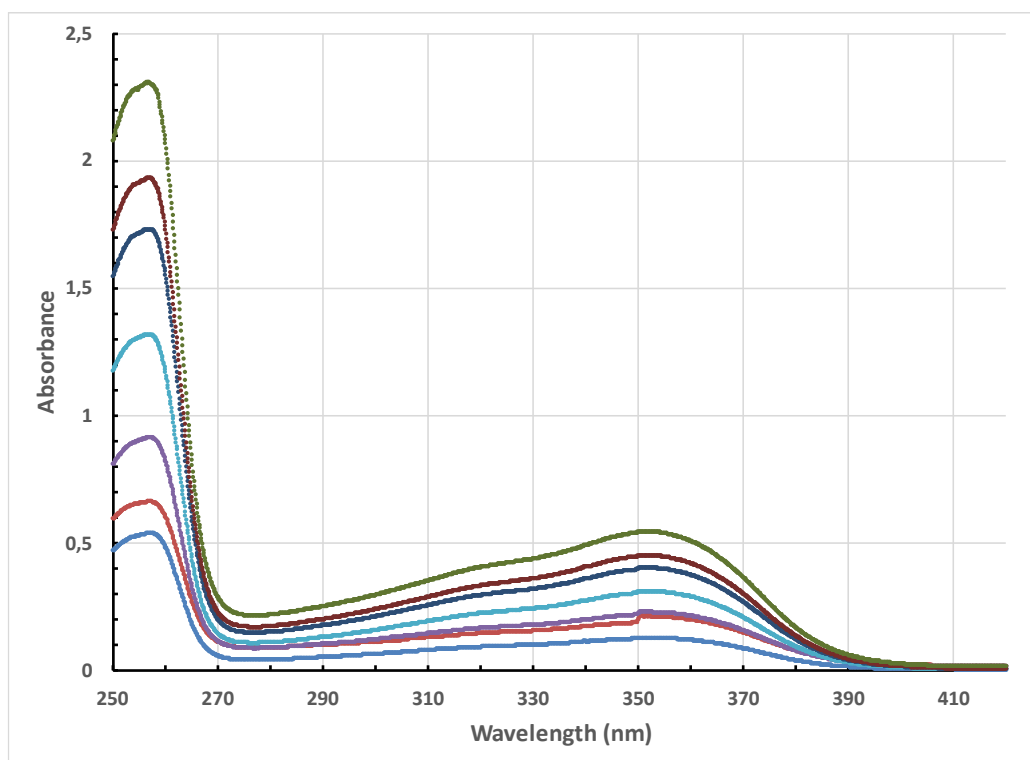


Figure 2. In the spectrum of absorbance against wavelength(nm) for 1,4, dihydroxy-2-naphthoic acid, two peaks were observed at 256 nm and 350 nm, which demonstrates that the concentration of 1,4, dihydroxy-2-naphthoic acid can be determined by absorbance measurements.

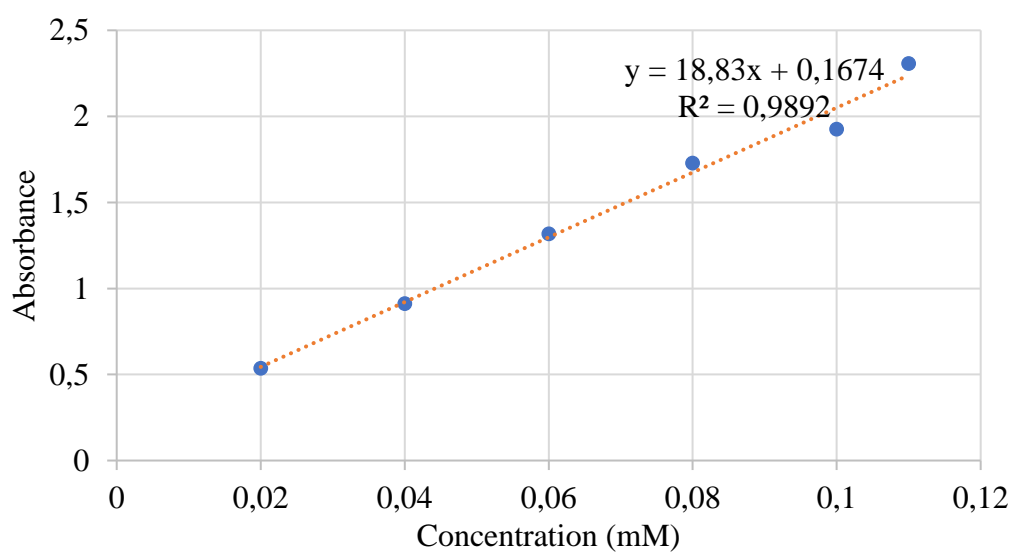
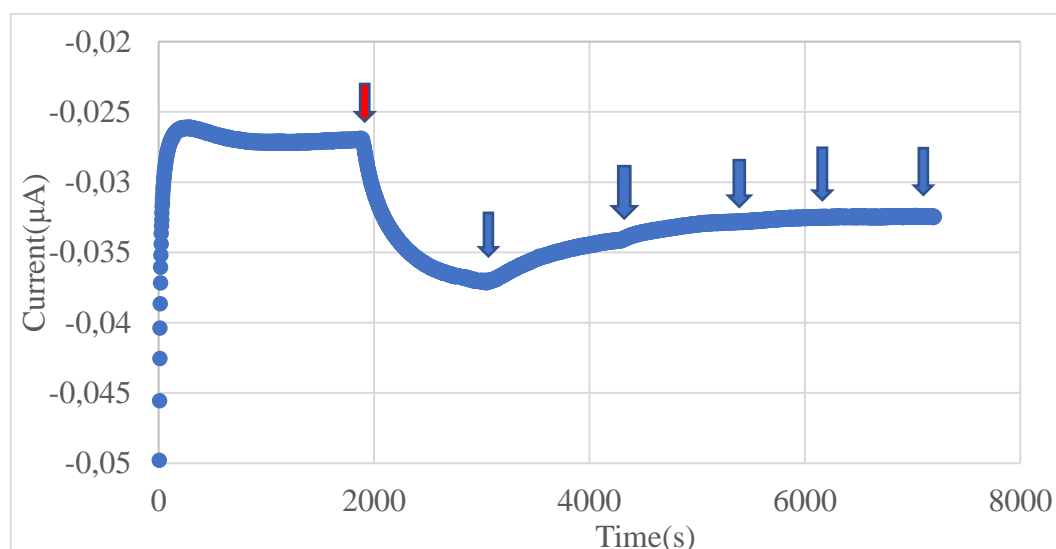
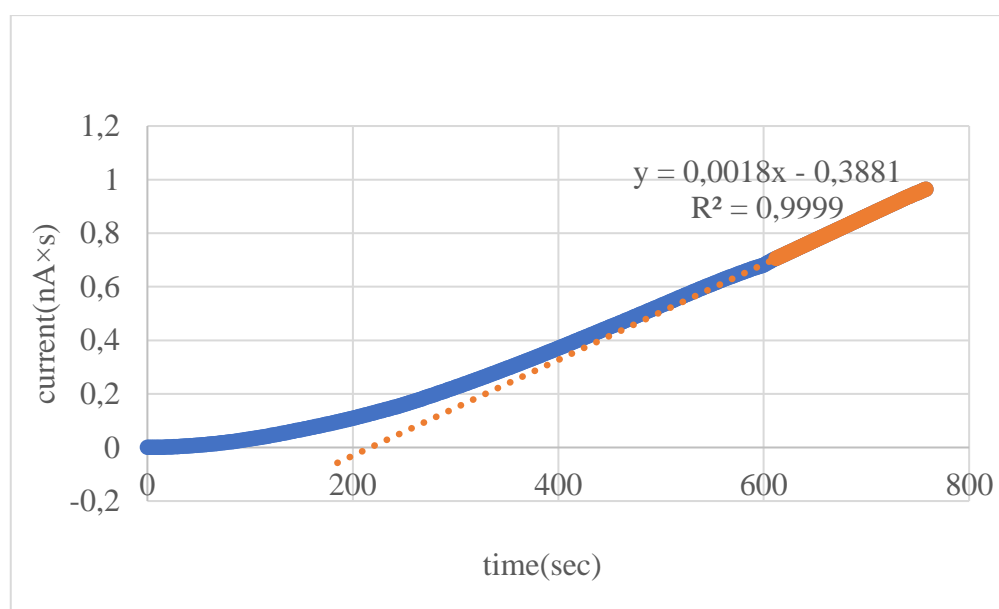


Figure 3. A spectrum of absorbance at 256 nm against concentration(mM) for 1,4-dihydroxy-2-naphthoic acid in PBS

## Determination of diffusion coefficients and lag times for hydrogen peroxide and 1,4-dihydroxy-2-naphthoic acid



**Figure 4.** A plot of current ( $\mu\text{A}$ ) against time(sec) recorded with skin covered oxygen electrode in PBS. Arrow in red indicates addition of 100  $\mu\text{L}$  of 100 mM hydrogen peroxide ( $\text{H}_2\text{O}_2$ ), resulting in 1mM in the measurement cell. The arrows in blue indicate five additions of 1,4-dihydroxy-2-naphthoic acid resulting in 0.02, 0.04, 0.06, 0.08 and 1.0 mM of this compound. Addition of hydrogen peroxide results in an increase in current responses and a decrease in current response is observed when 1,4-dihydroxy-2-naphthoic acid is pipetted into the electrochemical cell containing PBS and 5mM EDTA.



**Figure 5.** A plot of integral of current ( $\text{nA} \times \text{s}$ ) against time(s) recorded with skin covered oxygen electrode in PBS for the estimation of lag time and diffusion coefficient for hydrogen peroxide after amperometric measurements with skin covered oxygen electrode.

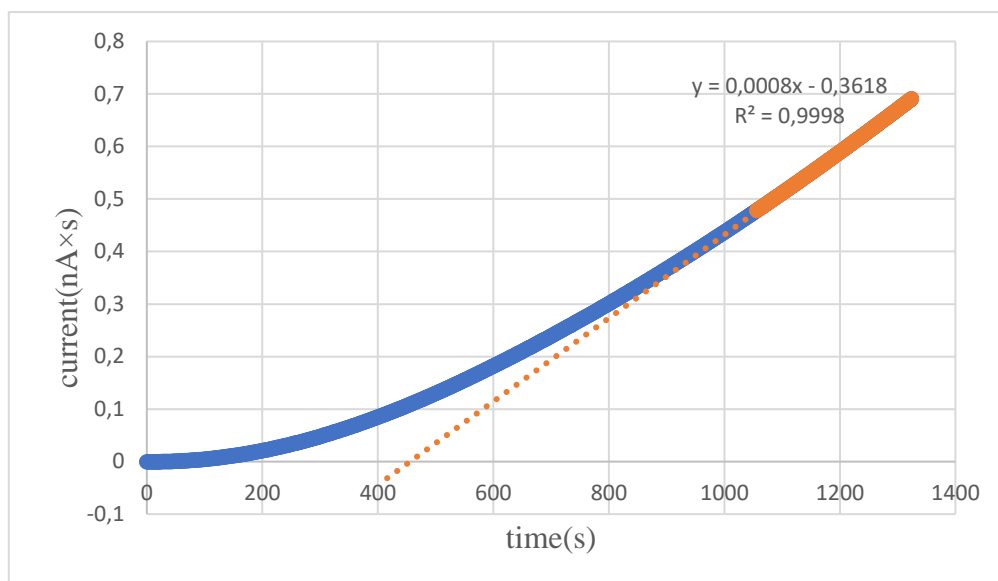


*Figure 6.* A plot of integral of current (nA×s) against time(s) recorded with skin covered oxygen electrode in PBS for the estimation of lag time and diffusion coefficients for 1,4- dihydroxy-2-naphthoic acid after amperometric measurements with skin covered oxygen electrode.

*Table 3.* A table with the estimated lag times and diffusion coefficients for hydrogen peroxide using skin covered oxygen electrode in PBS. The experiment was performed three times.

Experiments	1	2	3	Mean	Standard deviation
Lag-time(s)	159.1	215.6	253.6	209s	± 39 s
Diffusion co-efficient(cm <sup>2</sup> /s)	1.05×10 <sup>-9</sup>	7.7×10 <sup>-10</sup>	6.6×10 <sup>-10</sup>	9.7×10 <sup>-10</sup>	± 3.6×10 <sup>-10</sup> cm <sup>2</sup> /s

**Table 4.** A table with estimated lag times and diffusion coefficients for 1,4-dihydroxy-2-naphthoic acid using skin covered oxygen electrode in PBS. The experiment was performed three times.

	1	2	3	Mean	Standard deviation
Lag-time(s)	161	452	388	334	$\pm 124$ s
Diffusion co-efficient( $\text{cm}^2/\text{s}$ )	$1.0 \times 10^{-9}$	$3.7 \times 10^{-10}$	$4.3 \times 10^{-10}$	$6.1 \times 10^{-10}$	$\pm 3.0 \times 10^{-10}$ $\text{cm}^2/\text{s}$

#### Determination of Michaelis-Menten constants for hydrogen peroxide and 1,4-dihydroxy-2 naphthoic acid

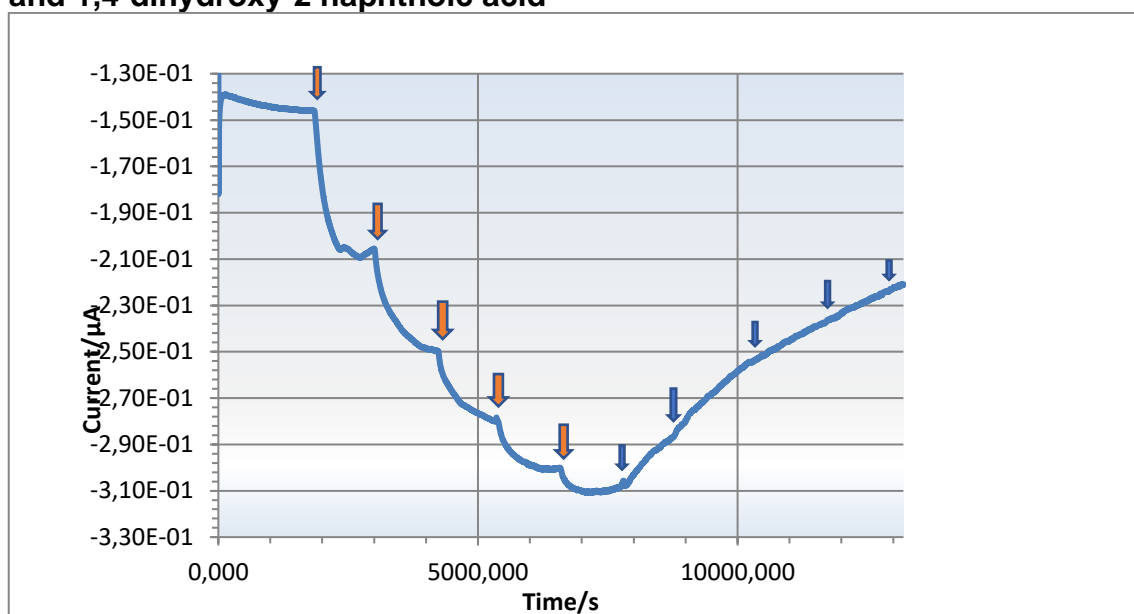


**Figure 7.** A plot of current ( $\mu\text{A}$ ) against time recorded with skin covered electrode in PBS. Arrows in red indicate five additions of  $100 \mu\text{L}$  of  $100 \text{ mM}$  hydrogen peroxide ( $\text{H}_2\text{O}_2$ ) and arrows in blue indicate five additions of  $100 \mu\text{L}$  of  $2 \text{ mM}$  1,4-dihydroxy-2-naphthoic acid resulting in  $0.02$ ,  $0.04$ ,  $0.06$ ,  $0.08$  and  $1.0 \text{ mM}$  of this compound. Addition of hydrogen peroxide results in an increase in current responses and a decrease in current response is observed when 1,4-dihydroxy-2-naphthoic acid is pipetted into the electrochemical cell.

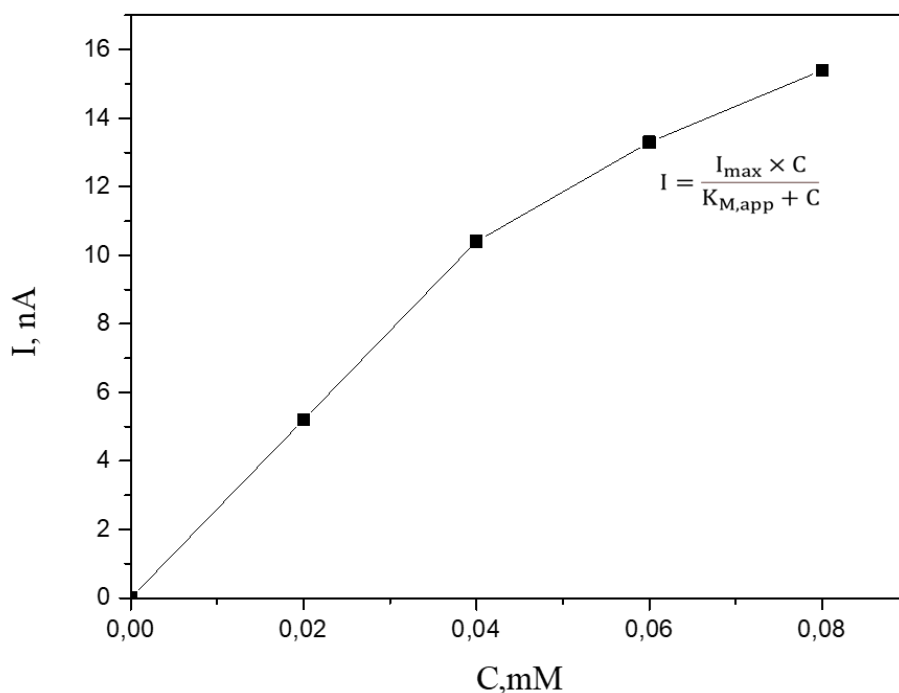


Figure 8. A plot of current response (nA) against concentrations(mM) for 1,4-dihydroxy-2-naphthoic acid. The equation  $I = \frac{I_{max} \cdot C}{K_{M,app} + C}$  was used to estimate apparent Michaelis-Menten constant ( $K_{M,app}$ ) which is the concentration of the substrate, 1,4-dihydroxy-2-naphthoic at half of the maximum current of the reaction,  $I_{max}$ .

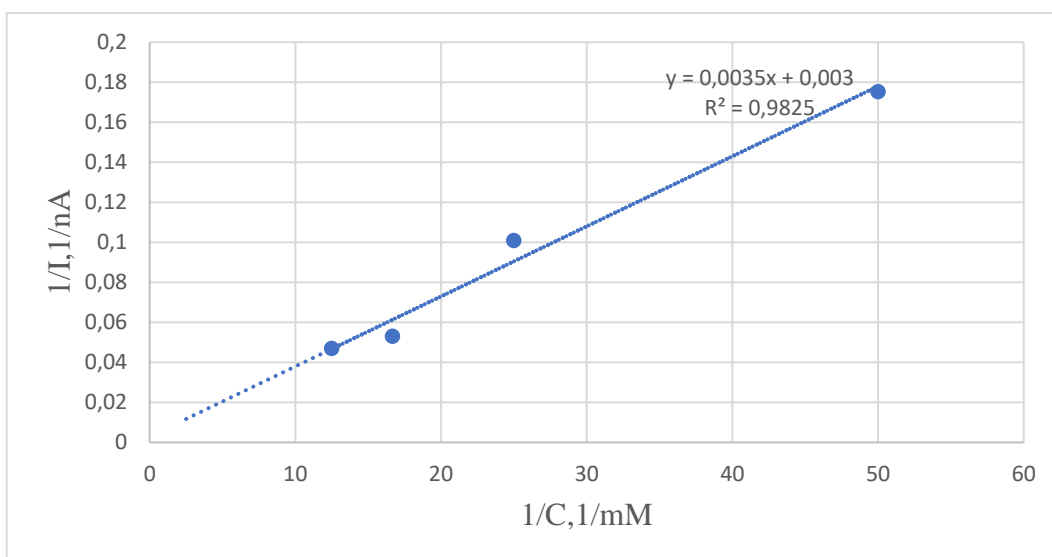
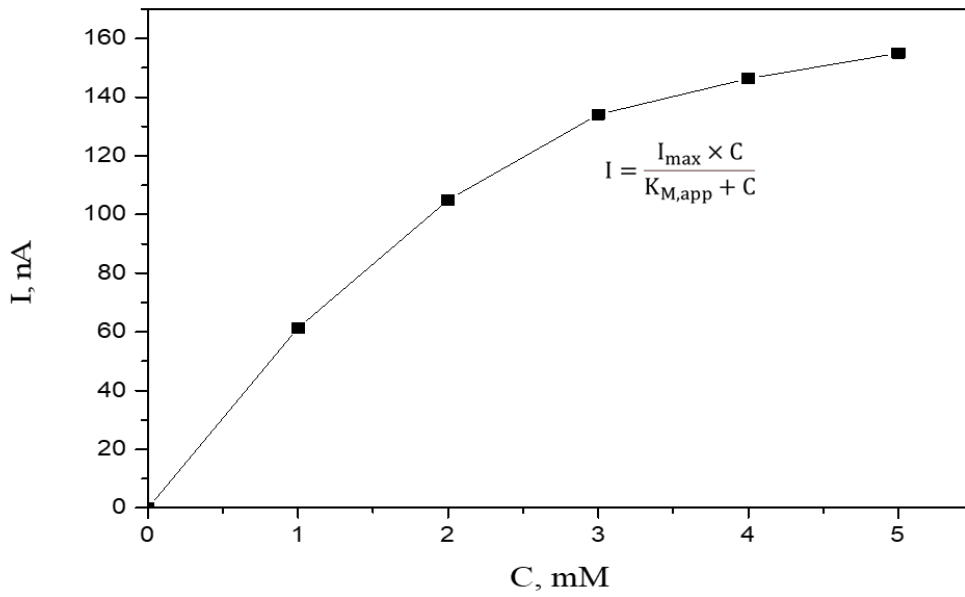
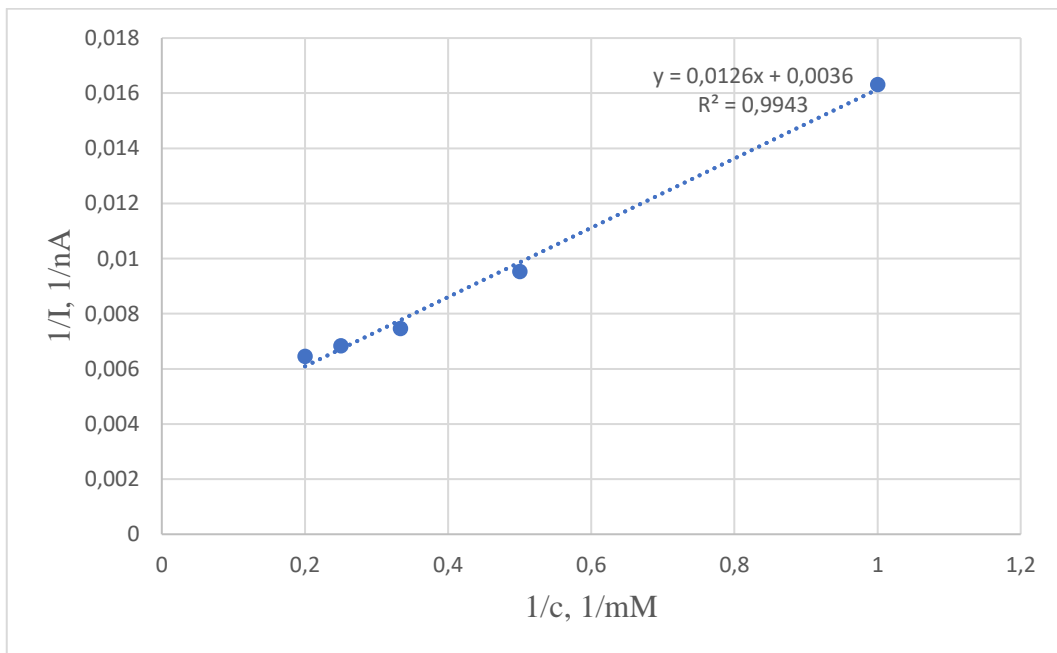


Figure 9. A plot of inverse of current(1/nA) against inverse of concentration(1/mM) for 1,4-dihydroxy-2-naphthoic acid following a rearrangement of equation I gives the linear equation  $\frac{1}{I} = \frac{K_{M,app} \times 1}{I_{max} \times C} + \frac{1}{I_{max}}$  from which  $K_{M,app}$  and  $I_{max}$  can also be estimated using data collected with skin covered oxygen electrode setup.



*Figure 10.* A plot of current response (nA) against concentrations(mM) for hydrogen peroxide. The equation  $I = \frac{I_{max} \cdot c}{K_{M,app} + c}$  was used to estimate apparent Michaelis-Menten constant ( $K_{M,app}$ ) which is the concentration of the substrate, hydrogen peroxide at half of the maximum current of the reaction,  $I_{max}$ .



*Figure 11.* A plot of inverse of current(1/nA) against inverse of concentration(1/mM) for hydrogen peroxide following a rearrangement of the equation I gives the linear equation  $\frac{1}{I} = \frac{K_{M,app} \times 1}{I_{max} \times C} + \frac{1}{I_{max}}$  from which  $K_{M,app}$  and  $I_{max}$  can also be estimated using data collected with skin covered oxygen electrode setup.

*Table 5.* A table with estimated  $I_{\max}$  and  $K_{M,app}$  for 1,4-dihydroxy-2-naphthoic acid following skin covered oxygen electrode in PBS. Experiment was performed three times.

	1	2	3	Mean	Standard deviation
$I_{\max}$	125	58	333	172 nA	$\pm 117$ nA
	1	2	3	Mean	Standard deviation
$K_{M,app}$	0.16	0.20	1.16	0.51 mM	$\pm 0.46$ mM

*Table 6.* A table with estimated  $I_{\max}$  and  $K_{M,app}$  for hydrogen peroxide following skin covered oxygen electrode in PBS. Experiment was performed three times.

	1	2	3	mean	Standard deviation
$I_{\max}$	277	60	1250	529 nA	$\pm 517$ nA
	1	2	3	mean	Standard deviation
$K_{M,app}$	3.5	7.1	15.5	8.7 mM	$\pm 5.0$ mM



### Determination of flux

After 4hr penetration experiment absorbance at 256 nm was 0.087. Using this value the concentration can be calculated.

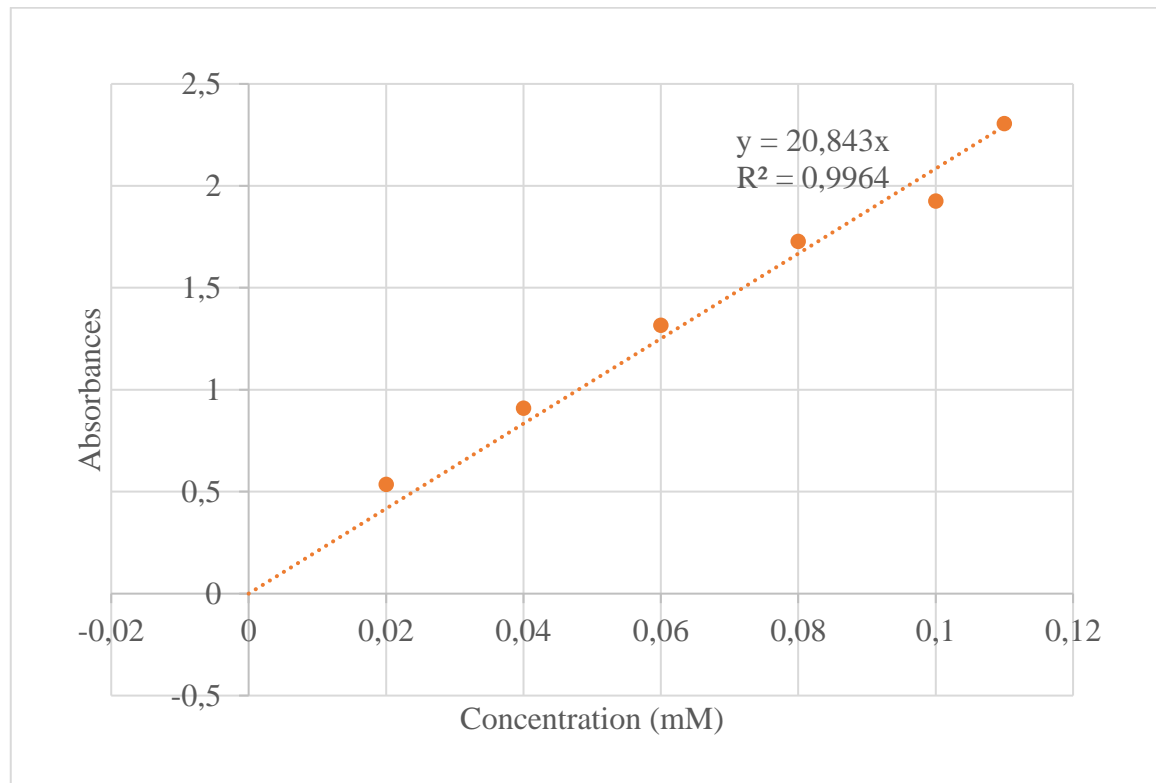


*Figure 12.* A calibration plot of absorbance at 256 nm against concentration(mM) for 1,4 dihydroxy-2-naphthoic acid with equation of the line,  $y = 20.843x$  where intercept was set to zero,  $b=0$  i.e.,  $y = ax$  is a calibration line, where  $x$  is concentration in mM and  $y$  is absorption at 256 nm.

Absorbance at 256 nm is deducted from absorbance at 331 nm due to background signal

$$\text{i.e., } 0.063 - 0.002 = 0.061$$

from equation of the line,  $y=20.843x$

when  $y$  is 0.061, then  $0.061 = 20.843x$

$$x = 0.00292 \text{ mM}$$

At  $t = 0$ , number of moles in donor chamber = concentration  $\times$  volume

$$\text{i.e., } 2 \text{ mM} \times 0.6 \text{ mL} = 1.2 \text{ } \mu\text{moles}$$

At  $t = 0$ , number of moles in receptor chamber = concentration  $\times$  volume

$$\text{i.e., } 0 \text{ mM} \times 6 \text{ mL} = 0 \text{ } \mu\text{moles}$$

At  $t = 4$  hrs, number of moles in receptor chamber = concentration  $\times$  volume

i.e.,  $0.00292 \text{ mM} \times 6 \text{ mL} = 0.0175 \text{ } \mu\text{moles}$

Flux is calculated taking into account concentration in receptor chamber

$$\text{Flux} = \frac{\Delta n}{t \times \text{area of skin.}} = \frac{(n_{t=4h} - n_{t=0h})}{t \times \text{area of skin.}}$$

where n is amount of 1,4-dihydroxy-naphthoic acid in receptor chamber at 4 hr (14400 s) or 0 hr as indicated by subscript. Area of 0.9 cm diameter skin is equal to  $0.636 \times 10^{-4} \text{ m}^2$ .

$$\text{Flux} = \frac{[0.0175 - 0] \text{ } \mu\text{moles}}{14.4 \cdot 10^3 \text{ s} \times 0.636 \cdot 10^{-4} \text{ m}^{-2}} = 0.0191 \text{ } \mu\text{mol s}^{-1} \text{ m}^{-2}$$

Therefore flux =  $0.0639 \pm 0.0575 \text{ } \mu\text{mol s}^{-1} \text{ m}^{-2}$  (This is the mean and standard deviation from three replicates).

## DISCUSSION

Considering the immense benefits of vitamin K4 in the body it is of relevance to study its interaction and permeability with the skin. In this thesis the permeability, topical and transdermal delivery of vitamin K4 was studied with amperometry measurements using skin covered oxygen electrode and Franz diffusion cell set up. For vitamin K to be used for treatment of dark circles and pigments under the eye it has to penetrate the stratum corneum, thickness 10-20  $\mu\text{m}$  (Zorec et al., 2015). The structure of the stratum corneum can be described as a brick-and-mortar formation with layers of 15-20 corneocytes embedded within a lipid matrix (Walicka and Iwanowska-Chomiak, 2018). This lipid matrix has been found to characterize the main barrier to diffusion of substances (De Jager et al., 2006) and a significant reduction in stratum corneum lipid composition and organization has been investigated to be an underlying factor for a defective barrier function and several skin diseases (Yamamoto et al., 1991).

Amperometric measurements were conducted using a skin covered oxygen electrode as an in-vitro tool to investigate the permeability of 1,4-dihydroxy-2-naphthoic acid, a model of vitamin K4. The skin covered oxygen electrode was immersed into PBS solution with 1mM  $\text{H}_2\text{O}_2$  that diffused into the skin membrane (Eskandari et al., 2019) where  $\text{O}_2$  was generated by the catalase reaction,  $\text{H}_2\text{O}_2 + \text{H}_2\text{O}_2 \xrightarrow{\text{catalase}} \text{O}_2 + 2\text{H}_2\text{O}$ . The generated  $\text{O}_2$  is reduced at the surface of the platinum electrode resulting in an increase in reduction current response as evident in figure 3 (the reduction current has a negative sign by definition). Addition of 100  $\mu\text{L}$  of 1,4-dihydroxy-2-naphthoic acid as an antioxidant reacts with  $\text{H}_2\text{O}_2$  and minimizing substrate concentration hence resulting in a decrease in current response as evident in figure 4. The current responses which occurs when catalase in the skin converts  $2\text{H}_2\text{O}_2$  into  $\text{O}_2$  reflects the penetration of both  $\text{H}_2\text{O}_2$  and 1,4-dihydroxy-2-naphthoic acid in the skin. Penetration of solutes through the

skin depends on the physicochemical properties of the solute (Ng and Lau, 2015). Solutes with molecular weights < 500 Da with log P between 1 and 3 penetrates easily through the skin (Alkilani et al., 2015). Diffusion coefficients from table 3 and table 4 for H<sub>2</sub>O<sub>2</sub> and 1,4-dihydroxy-2-naphthoic acid respectively were estimated from lag-times of current responses following skin covered oxygen electrode. Lag times were estimated to be  $209 \pm 39$  and  $334 \pm 125$  sec for H<sub>2</sub>O<sub>2</sub> and 1,4-dihydroxy-2-naphthoic acid respectively. The diffusion coefficient of 1,4-dihydroxy-2-naphthoic acid,  $6.1(\pm 3.0) \times 10^{-10} \text{ cm}^2/\text{s}$  is lower than that of H<sub>2</sub>O<sub>2</sub>, suggesting a slower penetration of 1,4-dihydroxy-2-naphthoic acid through the skin. This result is anticipated since 1,4-dihydroxy-2-naphthoic acid has a higher molecular weight, 204.18g/mol than H<sub>2</sub>O<sub>2</sub>, molecular weight 34.0147g/mol. 1,4-dihydroxy-2-naphthoic acid is very lipophilic since it has a log P of 2.5 and a molecular weight lower than 500 Da penetration through the skin occurs through the intercellular pathway by free volume diffusion mechanism.

The skin covered oxygen electrode is a suitable in-vitro setup to study the concept of the Michaelis-Menten equation which is applicable in the study of enzymatic reactions at different substrate concentrations (Berglund et al., 2020). From figure 7 each addition of 100  $\mu\text{L}$  H<sub>2</sub>O<sub>2</sub> resulted in an increase in reduction current responses as oxygen generated in the catalase reaction is reduced at the surface of the platinum electrode. Each addition of 100  $\mu\text{L}$  of 1,4-dihydroxy-2-naphthoic acid depletes some H<sub>2</sub>O<sub>2</sub> subsequently minimizing the amount of O<sub>2</sub> generated thus resulting in a decrease in current response. The Michaelis-Menten phenomenon can be applied to describe non-linear pharmacokinetics (Van Ginneken and Russel, 1989). Non-linear pharmacokinetics occurs due to saturation of elimination system which yields changes in clearance of drugs (Birkett, 1994). Drug elimination kinetics changes from first order to zero order with increasing dose. Most drugs with few exceptions undergo elimination by first order kinetics (Borowy and Ashurst, 2018). Michaelis-Menten constant can be predicted from plots of rates of reaction against concentrations of substrate. From such plots V<sub>max</sub> which characterizes the maximum rate of the reaction can also be predicted. A representation of such plot is seen in figures 8 and 10 for hydrogen peroxide and 1,4-dihydroxy-2-naphthoic acid respectively where current(nA) has been plotted as a function of concentrations of substrate(mM) which is H<sub>2</sub>O<sub>2</sub> and 1,4-dihydroxy-2-naphthoic in this study. From table 5 K<sub>M, app</sub> was estimated to be  $0.51 \pm 0.46$  mM with I<sub>max</sub> of  $172.27 \pm 117.08$  nA for 1,4-dihydroxy-2-naphthoic acid. Assuming 1,4-dihydroxy-2-naphthoic acid undergoes non-linear pharmacokinetics, it is likely that at a concentration above 0.51 mM elimination will follow zero order kinetics. Generally elimination of 1,4-dihydroxy-2-naphthoic acid from circulation will be dependent on time regardless of plasma concentration. (Birkett, 1994, Borowy and Ashurst, 2018). This can result in drug accumulation without a continual monitoring of plasma concentrations. Contrarily, at concentrations below 0.51 mM elimination follows first order kinetics where a constant proportion of 1,4-dihydroxy-2-naphthoic acid will be eliminated depending on plasma concentration (ibid). Taking into consideration the experimentally determined K<sub>M, app</sub> for 1,4-dihydroxy-2-naphthoic acid dose of formulations for clinical application should not result in plasma concentrations far higher than 0.51 mM since one may be approaching the toxicity range. From table 6 K<sub>M, app</sub> and I<sub>max</sub> were estimated to be  $8.7 \pm 5.0$  mM and  $529.59 \pm 517.04$  nA respectively for H<sub>2</sub>O<sub>2</sub>. Similarly if H<sub>2</sub>O<sub>2</sub> exhibits non-

linear pharmacokinetics, the above principle will be observed with concentrations above and below  $11.5 \pm 3.4$  mM.

As a selective permeable barrier the skin allows molecules to permeate through at different rates (Ng and Lau, 2015). Flux, a parameter which assess the amount of solute permeated per area per unit time can be estimated by simple Franz cell procedure. Franz cell is a suitable in-vitro method to investigate penetration of solutes as it is a simple method and requires less amount of the solute for the study (Salamanca et al., 2018). Solubility of 1,4-dihydroxy-2-naphthoic acid was tested with PBS and 5 mM EDTA before permeability studies were conducted with Franz cell. A UV spectrophotometric assay was done to determine the concentration of 1,4-dihydroxy-2-naphthoic acid by measuring absorbances as seen in figure 2. Following UV spectrophotometric assay a calibration plot was obtained, figure 3, from which absorbances at 256 nm were extrapolated to determine the amount of 1,4-dihydroxy-2-naphthoic acid that had permeated through the stratum corneum into the receptor chamber at the 4<sup>th</sup> hour. The estimated concentration in the receptor chamber was then used for the determination of flux. In the Franz cell set up experimental conditions were kept constant with hourly sampling of 1,4-dihydroxy-2-naphthoic acid to read absorbances between 250 - 650 nm. The flux was experimentally estimated to be  $0.064 \pm 0.058 \mu\text{mols}^{-1}\text{m}^{-2}$  after 4 hours. This low flux value is expected as very lipophilic drugs such as vitamin K readily accumulates in the stratum corneum (Lopes et al., 2007). Due to the accumulation of vitamin K in the stratum corneum there is the need to develop different drug delivery mechanisms to ensure its delivery into systemic circulation (ibid) (Hutton et al., 2018). Theoretically the flux was estimated to be  $2 \times 10^{-12} \text{ molcm}^{-2}\text{s}^{-1}$  following the estimation of permeability constants using the four-penetration pathway model. This model allows to predict transdermal transport of solute through the skin (Mitragotri, 2003). Calculated values for permeability constants are presented in the appendix. Experimentally derived flux,  $0.064(\pm 0.05.8) \mu\text{mols}^{-1}\text{m}^{-2}$  was found to be higher than the theoretically derived flux and this is because the pig skin is more permeable than the human skin. All experiments were repeated in triplicates with supplementary figures presented in the appendix.

## CONCLUSION

The skin covered oxygen electrode has been demonstrated as an in-vitro tool for investigation of vitamin K4 model penetration and interaction at biobarriers. Current responses measured demonstrated the penetration and participation of vitamin K4 in redox reactions at biobarriers. The Michaelis-Menten constant allows one to understand and predict therapeutic levels of plasma concentrations and toxicity levels as well as elimination mechanisms to prevent adverse effects. Finally, Franz diffusion cell has been demonstrated to be a simple in-vitro technique for permeation studies of a vitamin K4 model. A further investigation will be to develop drug delivery procedures and strategies to facilitate transdermal drug delivery since vitamin K4 is a lipophilic drug and accumulates in the stratum corneum.

## **ACKNOWLEDGEMENTS**

I wish to express my sincere gratitude to the Almighty God for his mercies and goodness through my studies. I would like to extend my profound gratitude to my supervisor Professor Tautgirdas Ruzgas for his immense support through out this thesis project. My sincerest gratitude to Malmö University for the opportunity to acquire a higher education in the Biomedical Science programme. Lastly, I am grateful to my family and friends for their support and love throughout my studies.

## REFERENCES

- ALKILANI, A. Z., MCCRUDDEN, M. T. & DONNELLY, R. F. 2015. Transdermal drug delivery: innovative pharmaceutical developments based on disruption of the barrier properties of the stratum corneum. *Pharmaceutics*, 7, 438-470.
- BERGLUND, L. G., RISSANEN, S., JUSSILA, K., KAUFMAN, J. W., PIIRILÄ, P., SAVOLAINEN, K. M., KALLIOKOSKI, P., PASANEN, P., VILUKSELA, M. & LANDSTRÖM, U. 2020. *Physiological and toxicological considerations. Industrial Ventilation Design Guidebook*. United Kingdom: Academic Press.
- BIRKETT, D. 1994. Pharmacokinetics made easy 9: Non-linear pharmacokinetics. *Australian Prescriber*, 17.
- BOROWY, C. S. & ASHURST, J. V. 2018. *Physiology, Zero and First Order Kinetics*, Florida, StatPearls Publishing.
- DE JAGER, M., GROENINK, W., VAN DER SPEK, J., JANMAAT, C., GOORIS, G., PONEC, M. & BOUWSTRA, J. 2006. Preparation and characterization of a stratum corneum substitute for in vitro percutaneous penetration studies. *Biochimica et Biophysica Acta (BBA)-Biomembranes*, 1758, 636-644.
- ESKANDARI, M., REMBIESA, J., STARTAITÉ, L., HOLEFORS, A., VALANČIŪTĖ, A., FARIDBOD, F., GANJALI, M. R., ENGBLOM, J. & RUZGAS, T. 2019. Polyphenol-hydrogen peroxide reactions in skin: In vitro model relevant to study ROS reactions at inflammation. *Analytica chimica acta*, 1075, 91-97.
- GUSTAFSSON, B. E., DAFT, F. S., MCDANIEL, E. G., SMITH, J. C. & FITZGERALD, R. J. 1962. Effects of vitamin K-active compounds and intestinal microorganisms in vitamin K-deficient germfree rats. *The Journal of nutrition*, 78, 461-468.
- HILL, M. 1997. Intestinal flora and endogenous vitamin synthesis. *European journal of cancer prevention: the official journal of the European Cancer Prevention Organisation (ECP)*, 6, S43-5.
- HUTTON, A. R., QUINN, H. L., MCCAGUE, P. J., JARRAHIAN, C., REIN-WESTON, A., COFFEY, P. S., GERTH-GUYETTE, E., ZEHRUNG, D., LARRAÑETA, E. & DONNELLY, R. F. 2018. Transdermal delivery of vitamin K using dissolving microneedles for the prevention of vitamin K deficiency bleeding. *International journal of pharmaceutics*, 541, 56-63.
- LEBLANC, J. G., MILANI, C., DE GIORI, G. S., SESMA, F., VAN SINDEREN, D. & VENTURA, M. 2013. Bacteria as vitamin suppliers to their host: a gut microbiota perspective. *Current opinion in biotechnology*, 24, 160-168.
- LOPES, L. B., SPERETTA, F. F. & BENTLEY, M. V. L. 2007. Enhancement of skin penetration of vitamin K using monoolein-based liquid crystalline systems. *European Journal of Pharmaceutical Sciences*, 32, 209-215.
- MITRAGOTRI, S. 2003. *Modeling skin permeability to hydrophilic and hydrophobic solutes based on four permeation pathways*. *Journal of Controlled Release*, 86, 69-92.
- NG, K. W. & LAU, W. M. 2015. Skin deep: the basics of human skin structure and drug penetration. *Percutaneous penetration enhancers chemical methods in penetration enhancement*. New York City Springer.
- PANKAJA, N. 2016. *Biochemistry*, New Delhi, Jaypee brother's medical publishers.
- PAZYAR, N., HOUSHMAND, G., YAGHOUBI, R., HEMMATI, A. A., ZEINELI, Z. & GHORBANZADEH, B. 2019. Wound healing effects of topical Vitamin K: A randomized controlled trial. *Indian journal of pharmacology*, 51, 88.
- RAZZAQUE, M. S. 2011. Osteocalcin: a pivotal mediator or an innocent bystander in energy metabolism? *Nephrology Dialysis Transplantation*, 26, 42-45.

- ROWLAND, I., GIBSON, G., HEINKEN, A., SCOTT, K., SWANN, J., THIELE, I. & TUOHY, K. 2018. Gut microbiota functions: metabolism of nutrients and other food components. *European journal of nutrition*, 57, 1-24.
- SALAMANCA, C. H., BARRERA-OCAMPO, A., LASSO, J. C., CAMACHO, N. & YARCE, C. J. 2018. Franz diffusion cell approach for pre-formulation characterisation of ketoprofen semi-solid dosage forms. *Pharmaceutics*, 10, 148.
- SCHULTE, R., JORDAN, L. C., MORAD, A., NAFTEL, R. P., WELLONS III, J. C. & SIDONIO, R. 2014. Rise in late onset vitamin K deficiency bleeding in young infants because of omission or refusal of prophylaxis at birth. *Pediatric Neurology*, 50, 564-568.
- SCHURGERS, L. J. & VERMEER, C. 2000. Determination of phyloquinone and menaquinones in food. *Pathophysiology of Haemostasis and Thrombosis*, 30, 298-307.
- SHEARER, M. J. 2009. Vitamin K in parenteral nutrition. *Gastroenterology*, 137, S105-S118.
- VAN GINNEKEN, C. & RUSSEL, F. 1989. Saturable pharmacokinetics in the renal excretion of drugs. *Clinical pharmacokinetics*, 16, 38-54.
- WALICKA, A. & IWANOWSKA-CHOMIAK, B. 2018. Drug diffusion transport through human skin. *International Journal of Applied Mechanics and Engineering*, 23, 977-988.
- WORLD HEALTH ORGANIZATION 2004. *Vitamin and mineral requirements in human nutrition*, Rome, World Health Organization.
- YAMAMOTO, A., SERIZAWA, S., ITO, M. & SATO, Y. 1991. Stratum corneum lipid abnormalities in atopic dermatitis. *Archives of dermatological research*, 283, 219-223.
- ZOREC, B., JELENC, J., MIKLAVČIČ, D. & PAVŠELJ, N. 2015. Ultrasound and electric pulses for transdermal drug delivery enhancement: Ex vivo assessment of methods with in vivo oriented experimental protocols. *International journal of pharmaceutics*, 490, 65-73.

# **APPENDIX**



FACULTY OF HEALTH  
AND SOCIETY

## **INVESTIGATION OF VITAMIN K INTERACTION AND TRANSDERMAL DELIVERY AT SKIN BARRIERS: STUDY USING K<sub>4</sub> MODEL**

ALBERTA AGYEMANG

Degree project in Biomedical science

120 credits

Biomedical surface science programme

August 2021

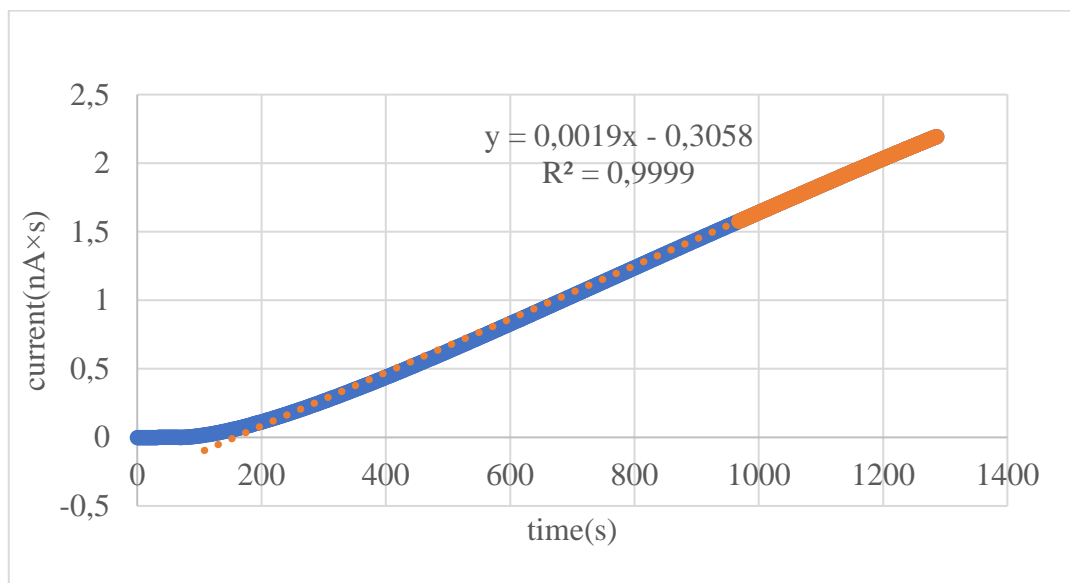
Malmö University

Health and Society

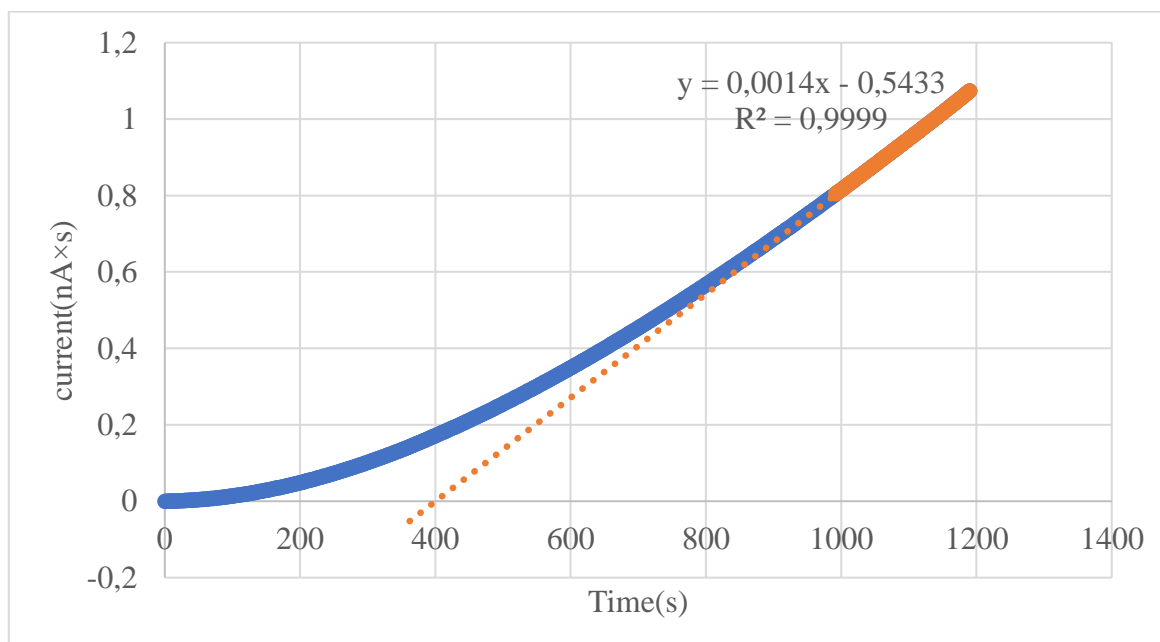
205 06 Malmö



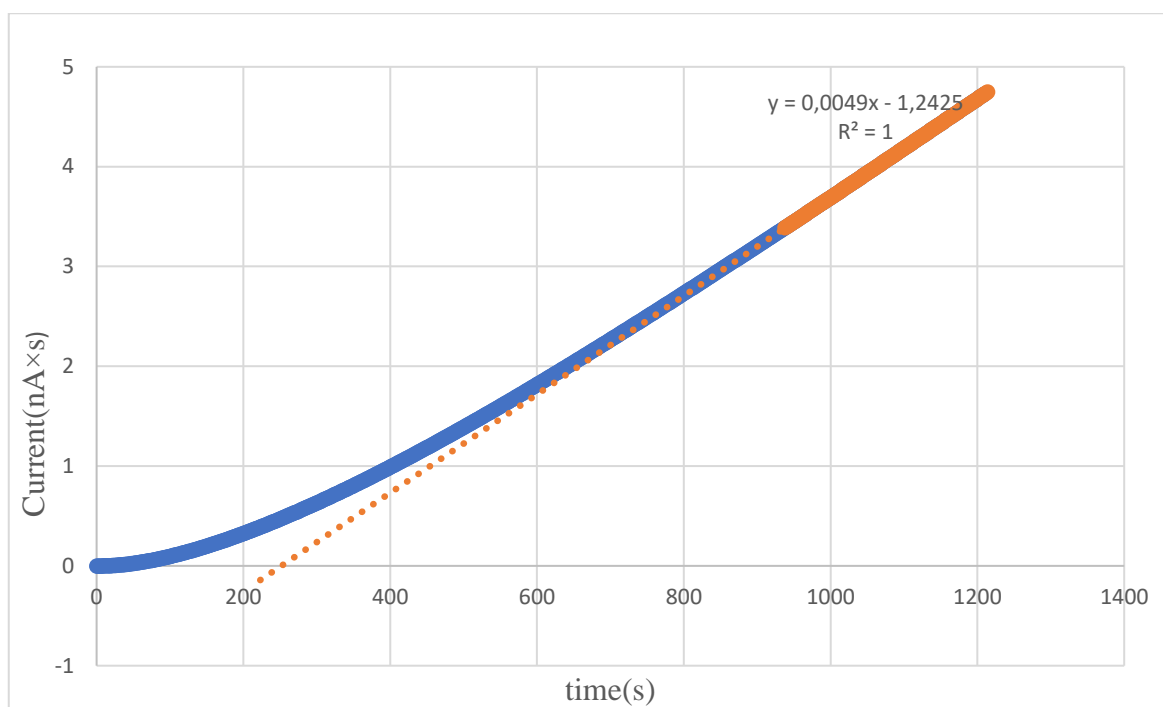
## Determination of lag times and diffusion coefficients



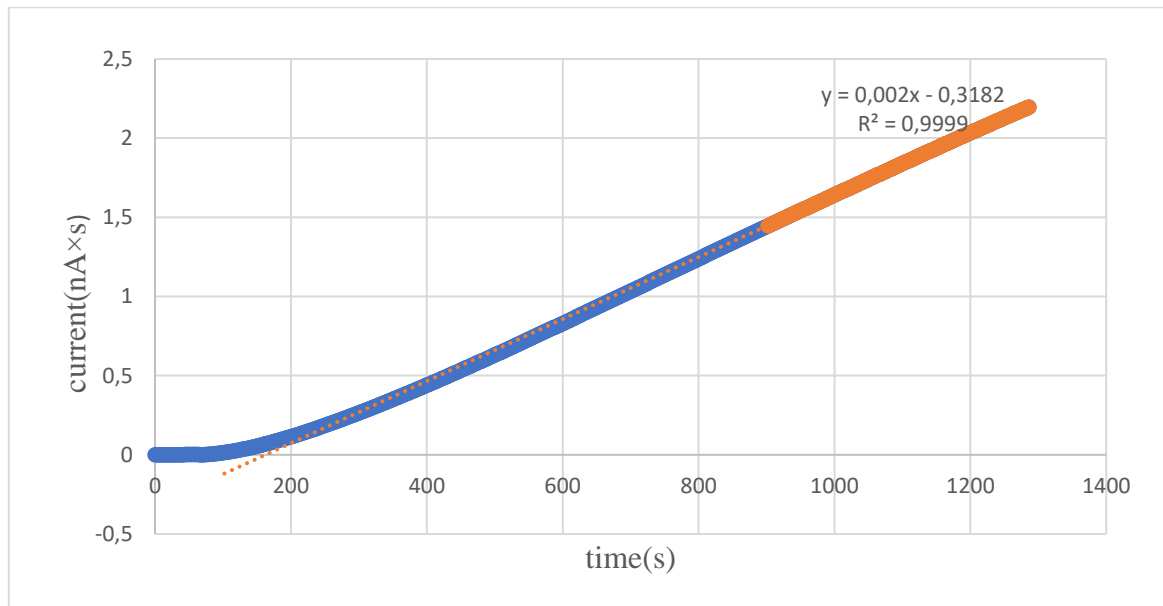
*Supplementary Figure 1.* A plot of integral of current (nA×s) against time(s) recorded with skin covered oxygen electrode in PBS for the estimation of lag time and diffusion coefficient for 1,4-dihydroxy-2-naphthoic acid after amperometric measurements with skin covered oxygen electrode.



*Supplementary Figure 2.* A plot of integral of current (nA×s) against time(s) recorded with skin covered oxygen electrode in PBS for the estimation of lag time and diffusion coefficient for 1,4-dihydroxy-2-naphthoic acid after amperometric measurements with skin covered oxygen electrode.

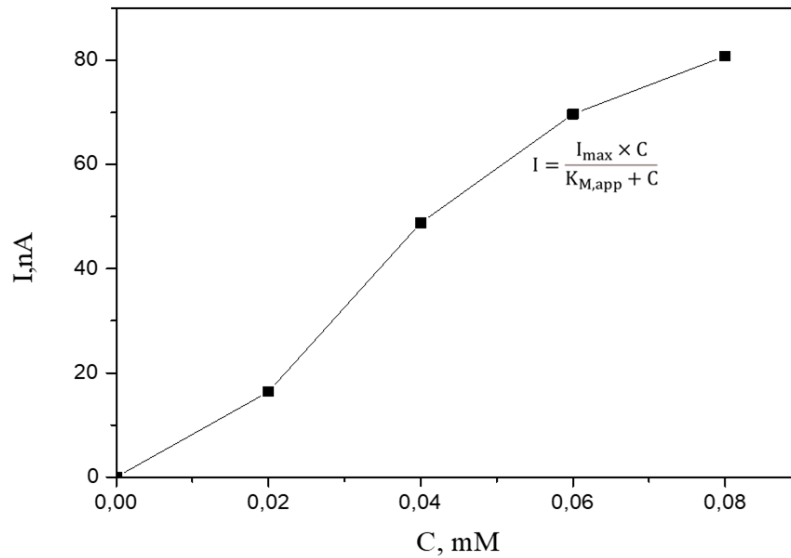


*Supplementary Figure 3.* A plot of integral of current (nA×s) against time(s) recorded with skin covered oxygen electrode in PBS for the estimation of lag time and diffusion coefficient for hydrogen peroxide after amperometric measurements with skin covered oxygen electrode.

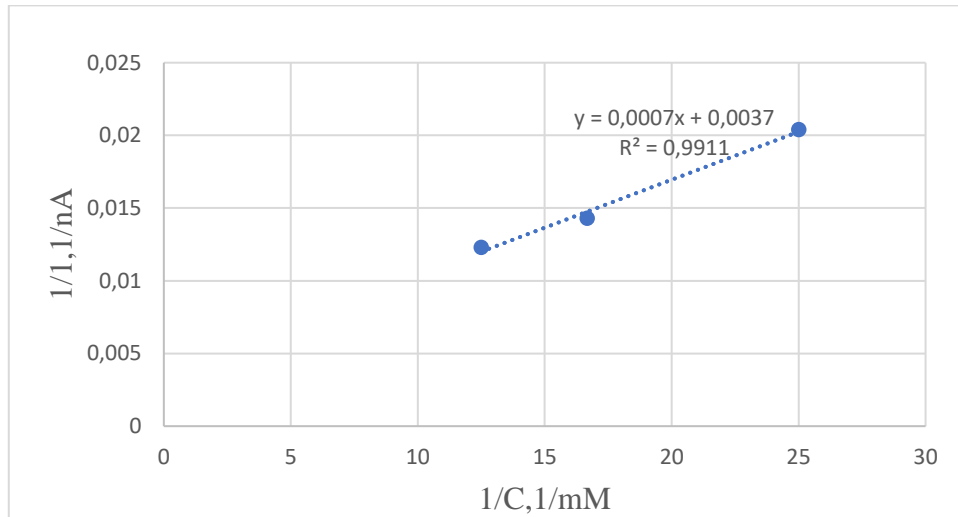


*Supplementary Figure 4.* A plot of integral of current (nA×s) against time(s) recorded with skin covered oxygen electrode in PBS for the estimation of lag time and diffusion coefficient for hydrogen peroxide after amperometric measurements with skin covered oxygen electrode.

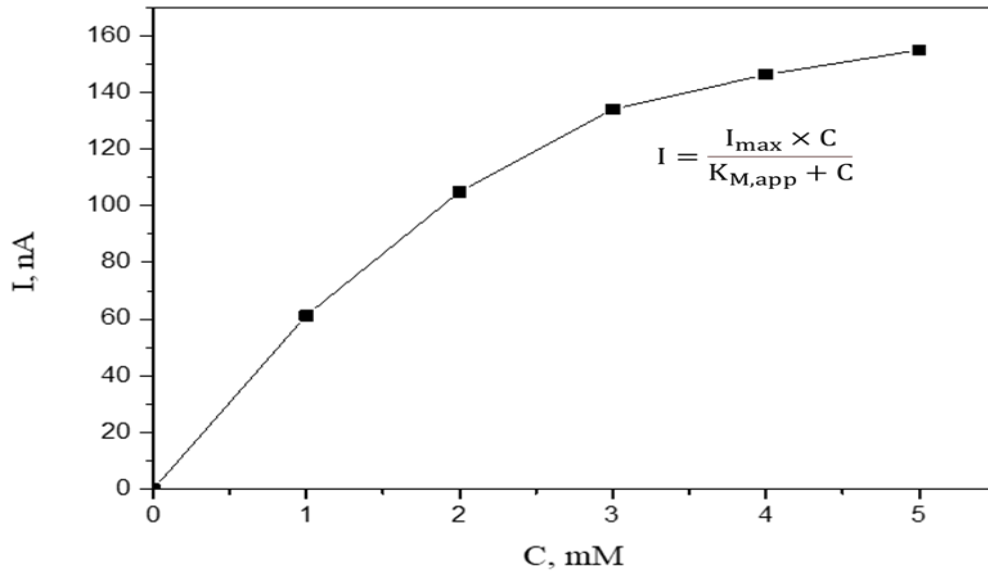
## Determination of Michaelis-Menten constants $K_{M, app}$



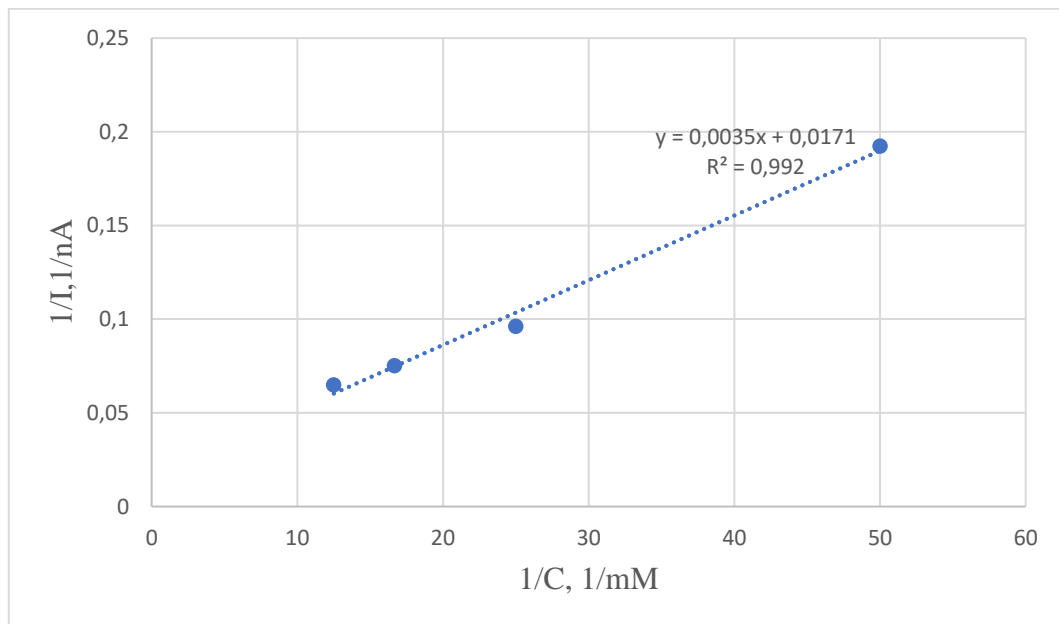
*Supplementary Figure 5.* A plot of current response (nA) against concentrations (mM) for 1,4-dihydroxy-2-naphthoic acid. The equation  $I = \frac{I_{max} \cdot C}{K_{M, app} + C}$  was used to estimate apparent Michaelis-Menten constant ( $K_{M, app}$ ) which is the concentration of the substrate, 1,4-dihydroxy-2-naphthoic at half of the maximum current of the reaction,  $I_{max}$ .



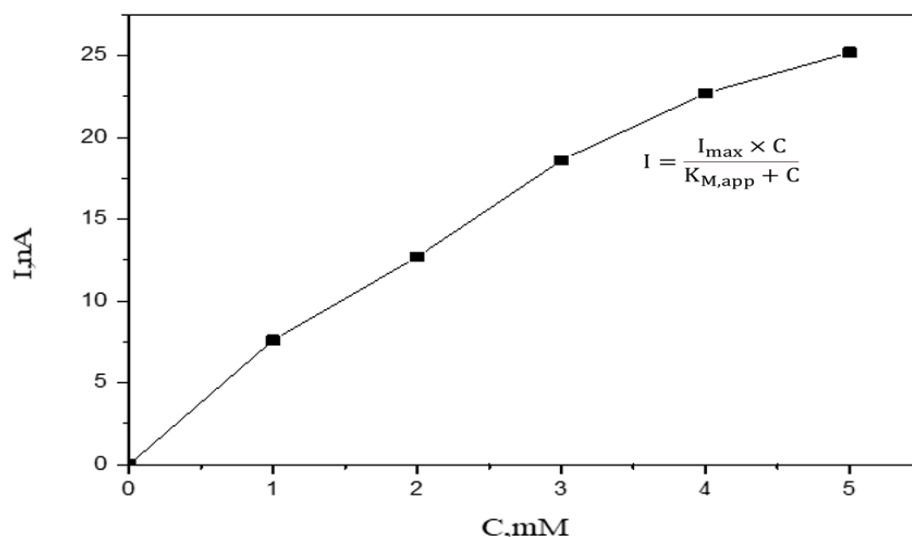
*Supplementary Figure 6.* A plot of inverse of current ( $1/nA$ ) against inverse of concentration ( $1/mM$ ) for 1,4-dihydroxy-2-naphthoic acid following a rearrangement of equation I gives the linear equation  $\frac{1}{I} = \frac{K_{M, app} \times 1}{I_{max} \times C} + \frac{1}{I_{max}}$  from which  $K_{M, app}$  and  $I_{max}$  can also be estimated using data collected with skin covered oxygen electrode setup.



*Supplementary Figure 7.* A plot of current response (nA) against concentrations(mM) for 1,4-dihydroxy-2-naphthoic acid. The equation  $I = \frac{I_{max} \cdot C}{K_{M,app} + C}$  was used to estimate apparent Michaelis-Menten constant ( $K_{M,app}$ ) which is the concentration of the substrate, 1,4-dihydroxy-2-naphthoic at half of the maximum current of the reaction,  $I_{max}$ .

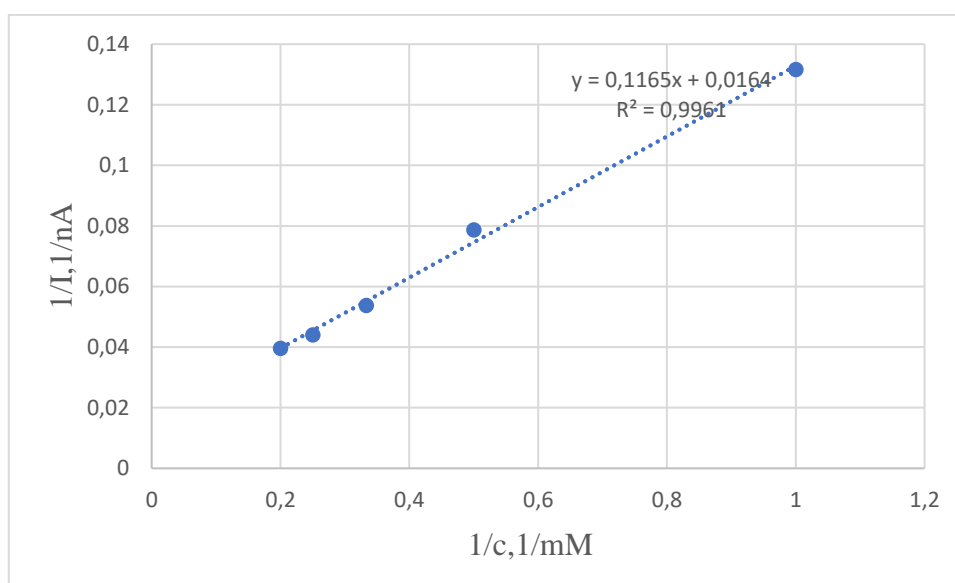


*Supplementary Figure 8.* A plot of inverse of current(1/nA) against inverse of concentration(1/mM) for 1,4-dihydroxy-2-naphthoic acid following a rearrangement of equation I gives the linear equation  $\frac{1}{I} = \frac{K_{M,app} \times 1}{I_{max} \times C} + \frac{1}{I_{max}}$  from which  $K_{M,app}$  and  $I_{max}$  can also be estimated using data collected with skin covered oxygen electrode setup.

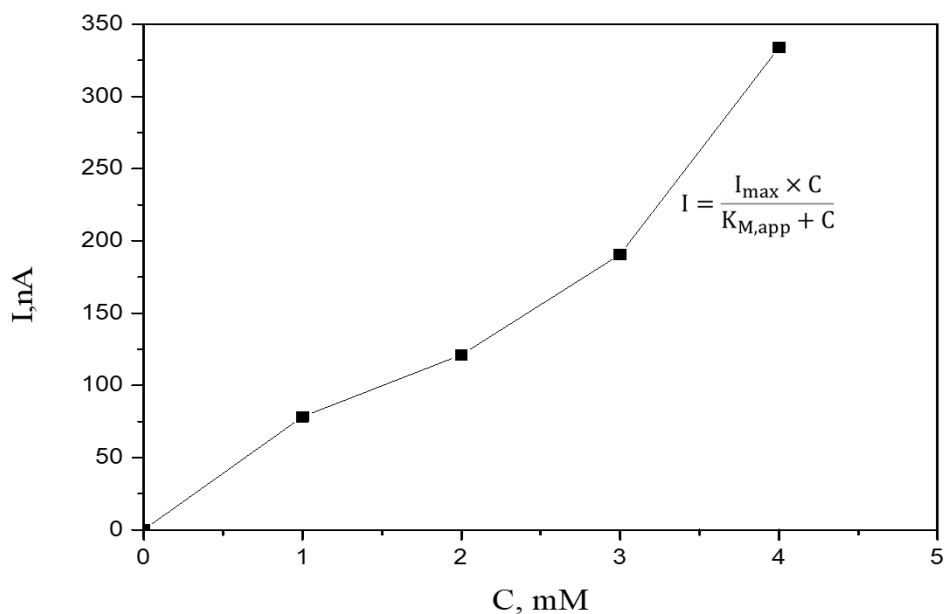


1

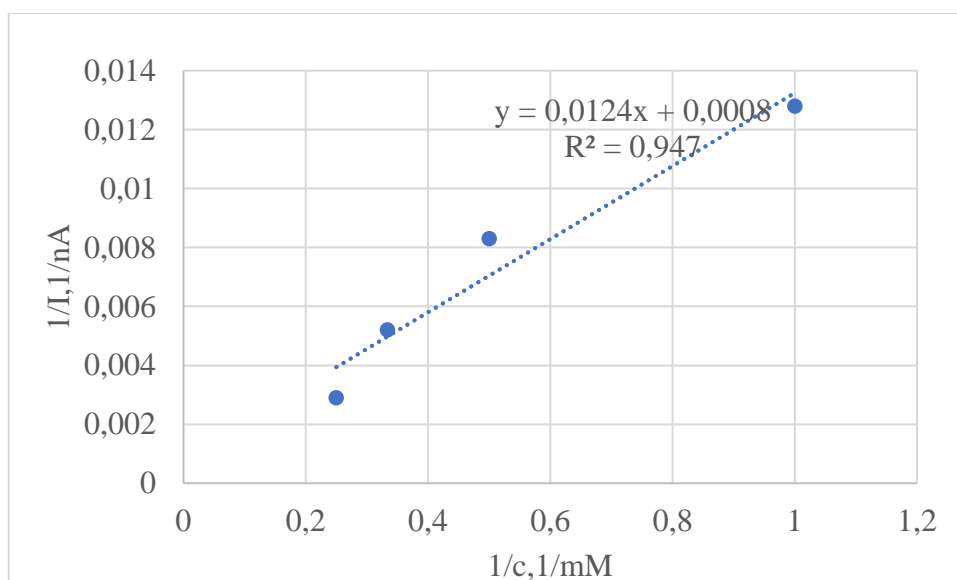
*Supplementary Figure 9.* A plot of current response (nA) against concentrations (mM) for hydrogen peroxide. The equation  $I = \frac{I_{max} \cdot C}{K_{M,app} + C}$  was used to estimate apparent Michaelis-Menten constant ( $K_{M,app}$ ) which is the concentration of the substrate, hydrogen peroxide at half of the maximum current of the reaction,  $I_{max}$ .



*Supplementary Figure 10.* A plot of inverse of current (1/nA) against inverse of concentration (1/mM) for hydrogen peroxide following a rearrangement of the equation I gives the equation  $\frac{1}{I} = \frac{K_{M,app} \times 1}{I_{max} \times C} + \frac{1}{I_{max}}$  from which  $K_{M,app}$  and  $I_{max}$  can also be estimated using data collected with skin covered oxygen electrode setup.



*Supplementary Figure 11.* A plot of current response (nA) against concentrations (mM) for hydrogen peroxide. The equation  $I = \frac{I_{max} \cdot C}{K_{M,app} + C}$  was used to estimate apparent Michaelis-Menten constant ( $K_{M,app}$ ) which is the concentration of the substrate, hydrogen peroxide at half of the maximum current of the reaction,  $I_{max}$ .



*Supplementary Figure 12.* A plot of inverse of current (1/nA) against inverse of concentration (1/mM) for hydrogen peroxide following a rearrangement of equation I gives the linear equation  $\frac{1}{I} = \frac{K_{M,app} \times 1}{I_{max} \times C} + \frac{1}{I_{max}}$  from which  $K_{M,app}$  and  $I_{max}$  can also be estimated using data collected with skin covered oxygen electrode setup

*Supplementary Table 1.* Estimated apparent Michaelis-Menten constants and current of maximum reaction with comments for hydrogen peroxide following skin covered oxygen electrode.

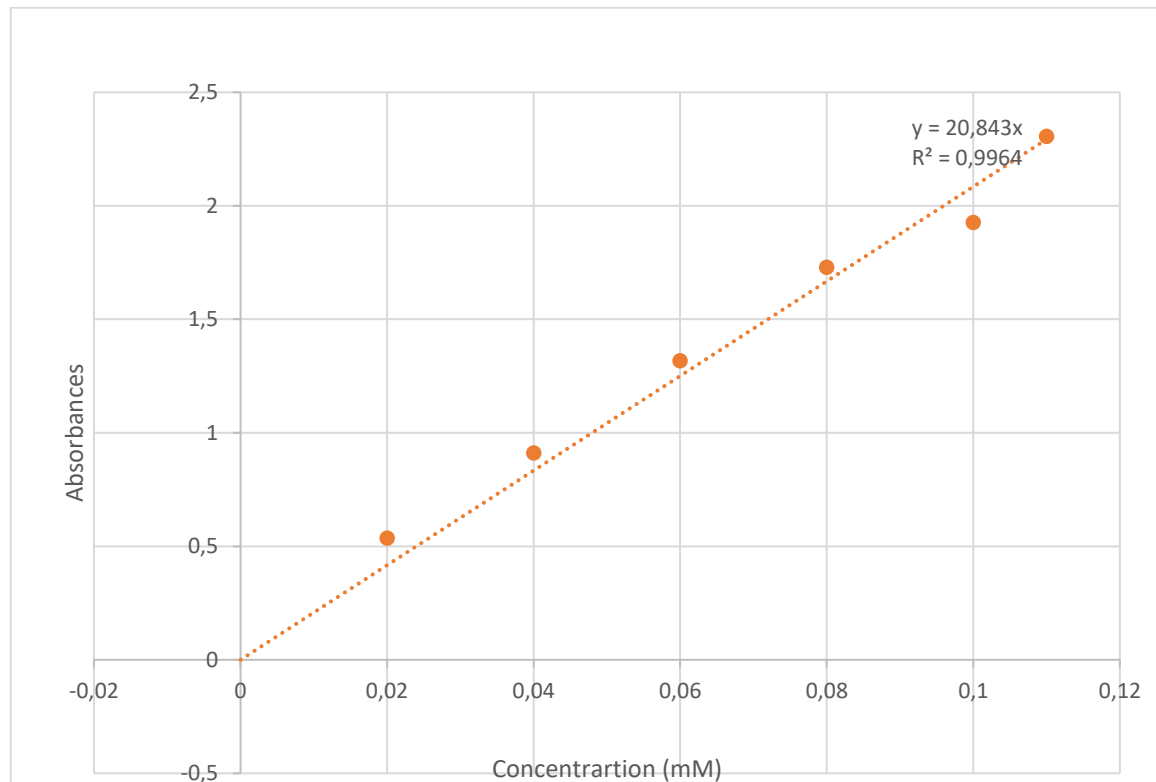
	Km	I <sub>max</sub>	Comments
Electrode 1	3.5	277	
Electrode 2	7.1	60	
Electrode 3	15.5	1250	The first point has been removed from the plot because intercept was negative.

*Supplementary Table 2.* Estimated apparent Michaelis-Menten constants and current of maximum reaction with comments for 1,4-dihydroxy-2-naphthoic acid following skin covered oxygen electrode.

	Km	I <sub>max</sub>	Comments
Electrode 1	0.16	125	
Electrode 2	0.45	120	The first point have been removed from the plot because the intercepts were negative
Electrode 3	2.50	714	

## Determination of flux

1. After 4hr penetration experiment absorbance at 256 nm was 0.087. Using this value we can calculate concentration



*Supplementary Figure 13.* A calibration plot of absorbance against concentration(mM) for 1,4 dihydroxy-2-naphthoic acid with equation of the line,  $y = 20.843x$  where intercept was set to zero,  $b=0$  i.e.  $y=ax$  is a calibration line, where  $x$  is concentration in mM and  $y$  is absorption at 256 nm.

2. After 4-hour penetration experiment absorbance at 256 nm was 0.462. Using this value, we can calculate concentration.

From equation of the line,  $y=20.843x$

when  $y$  is 0.462 then  $0.462 = 20.843x$

$$x = 0.0221 \text{ mM}$$

At  $t = 0$ , number of moles in donor chamber = concentration  $\times$  volume

$$\text{i.e., } 2\text{mM} \times 0.6\text{mL} = 1.2 \text{ moles}$$

At  $t = 0$ , number of moles in receptor chamber = concentration  $\times$  volume

$$\text{i.e., } 0 \text{ mM} \times 6 \text{ mL} = 0 \text{ moles}$$

At  $t = 4 \text{ hrs}$ , number of moles in receptor chamber = concentration  $\times$  volume

$$\text{i.e. } 0.0221\text{mM} \times 6\text{mL} = 0.1329 \text{ } \mu\text{moles}$$



$$\text{Flux} = \frac{\Delta n}{t \times \text{area of skin.}} = \frac{(n_{t=4h} - n_{t=0h})}{t \times \text{area of skin.}}$$

$$\text{Flux} = \frac{[0.1329 \times 0] \text{ moles}}{14.4 \cdot 10^3 \text{ s} \times 0.636 \cdot 10^{-4} \text{ m}^{-2}}$$

$$= 0.1451 \mu\text{mol s}^{-1} \text{m}^{-2}$$

3. After 4hr penetration experiment absorbance at 256 nm was 0.087. Using this value we can calculate concentration.

From equation of the line,  $y = 20.843x$

when  $y$  is 0.087 then  $0.087 = 20.843x$

$$x = 0.0042 \text{ mM}$$

At  $t = 0$ , number of moles in donor chamber = concentration  $\times$  volume

$$\text{i.e., } 2 \text{ mM} \times 0.6 \text{ mL} = 1.2 \text{ moles}$$

At  $t = 0$ , number of moles in receptor chamber = concentration  $\times$  volume

$$\text{i.e., } 0 \text{ mM} \times 6 \text{ mL} = 0 \text{ moles}$$

At  $t = 4 \text{ hrs}$ , number of moles in receptor chamber = concentration  $\times$  volume

$$\text{i.e., } 0.0042 \text{ mM} \times 6 \text{ mL} = 0.0252 \mu\text{moles}$$

$$\text{Flux} = \frac{\Delta n}{t \times \text{area of skin.}} =$$

$$\text{flux} = \frac{[0.0252 - 0] \text{ moles}}{14.4 \cdot 10^3 \text{ s} \times 0.636 \cdot 10^{-4} \text{ m}^{-2}}$$

$$= 0.0275 \mu\text{mol s}^{-1} \text{m}^{-2}$$

### Theoretical flux

Following the four-penetration pathway flux can be estimated using the equation below.

$$\text{Flux (molcm}^{-2}\text{s}^{-1}) = (K_p^{\text{fv}} + K_p^{\text{lateral}} + K_p^{\text{pore}} + K_p^{\text{shunt}}) * C \text{molcm}^{-3}$$

Where  $K_p^{\text{fv}}$  = free volume diffusion

$K_p^{\text{lateral}}$  = lateral diffusion of lipids.

$K_p^{\text{pore}}$  = diffusion through pores

$K_p^{\text{shunt}}$  = diffusion through shunts

$C$  = concentration of solute at surface of stratum corneum

1. Permeation of solute through free volume diffusion is suitable for hydrophobic solutes with molecular weight < 400Da

$$K_p^{fv} = \frac{D_b \cdot K_b}{\tau \cdot dsc}, \text{ where } D_b, \text{ diffusion coefficient in lipid bilayers} = 2.10^{-5} e^{-0.46r/r}$$

$$K_b, \text{ partition coefficient} \approx K_{O/W}^{0.7}$$

$\tau$ , tortiosity

dsc, thickness of stratum corneum.

To determine the radius,  $r[\text{\AA}]$  from  $D_b$ , it is calculated as:

$$\frac{4}{3}\pi r^3 = 0.9087 \cdot Mw[Da]$$

Mw of 1,4, dihydroxy-2-naphthoic acid = 204.18Da

$$\text{Therefore } r[\text{\AA}] = r^3 = \frac{2.7261 \times Mw}{4 \times 3.14}$$

$$r = 3.54$$

$$D_b = 2.10^{-5} e^{-5.76} = 6.3 \times 10^{-8} \text{ cm}^2 / \text{s}$$

To determine  $K_b$ , partition coefficient

$$K_b \approx K_{O/W}^{0.7}, K_{O/W}^{0.7} = 316.22$$

Therefore  $K_b = 56$

Substituting  $D_b$  and  $K_b$  into the equation,  $\frac{D_b \cdot K_b}{\tau \cdot dsc}$

$$K_p^{fv} = \frac{D_b \cdot K_b}{\tau \cdot dsc} = x = \frac{6.3 \times 10^{-8} \times 56}{3.6} = 9.8 \times 10^{-7} \text{ cms}^{-1}$$

2. Permeation of solute through lateral diffusion in lipid bilayers is suitable for hydrophobic solutes with molecular weight >400Da

$$K_p^{\text{lateral}} = \frac{D_b \cdot K_b}{\tau \cdot dsc}, \text{ where } D_b^{\text{lateral}} = 3 \times 10^{-9}$$

$$K_b = 56$$

$$T \cdot dsc = 3.6$$

$$K_p^{\text{lateral}} = \frac{3 \times 10^{-9} \times 56}{3.6} = 4.7 \times 10^{-8} \text{ cms}^{-1}$$

3. Diffusion of solutes through pores which is suitable for hydrophilic solutes

$$K_p^{\text{pore}} = 1.893 \times 10^{-8} \cdot r^{-0.6804}.$$

$R[\text{\AA}]$  has been determined to be 3.54

$$\text{Therefore, } K_p^{\text{pore}} = 1.893 \times 10^{-8} \times (3.54)^{-0.6804} = 8 \times 10^{-9} \text{ cms}^{-1}$$

4. Diffusion through shunts which is suitable for large hydrophilic solutes with molecular weight > 100KDa

$$K_p^{\text{shunt}} = 2 \times 10^{-9} \text{ cm s}^{-1}$$

$$\text{Therefore flux} = (K_p^{\text{fv}} + K_p^{\text{lateral}} + K_p^{\text{pore}} + K_p^{\text{shunt}}) * C \text{ mol cm}^{-3}$$

$$= (9.8 \times 10^{-7} \text{ cm s}^{-1} + 4.7 \times 10^{-8} \text{ cm s}^{-1} + 8 \times 10^{-9} \text{ cm s}^{-1} + 2 \times 10^{-9} \text{ cm s}^{-1}) * 2 \times 10^{-6}$$

$$= 2 \times 10^{-12} \text{ mol cm}^{-2} \text{ s}^{-1}$$